Int. j. adv. multidisc. res. stud. 2026; 6(1):58-61

Received: 17-11-2025
Accepted: 27-12-2025

International Journal of Advanced Multidisciplinary Research and Studies

ISSN: 2583-049X

Performance Evaluation of a Geiger-Müller Counter: Plateau Characteristics, Detection Efficiency, and Radiation Absorption Statistics

[1] Usman Abubakar, [2] Muttaka Umar, [3] Iliyasu Usman
[1, 2, 3] Department of Physics, Sokoto State University, P.M.B. 2134, Sokoto, Nigeria

Corresponding Author: **Muttaka Umar**

Abstract
Geiger-Müller (G-M) counters are fundamental in real-time radiation monitoring due to their portability and cost-effectiveness. This study systematically evaluates the operational parameters of a G-M counter system. Using a ^{137}Cs source, the operating voltage was determined to be 810 V within a stable plateau extending from 640 V to 980 V. Detection efficiency was assessed for various sources, yielding values of 0.003 % (^{210}Po), 0.08 % (^{90}Sr), and 0.02 % (^{60}Co), with low values attributed to gas density constraints. Radiation attenuation studies confirmed that absorption cross-sections are highly dependent on the atomic number (Z) of the shielding material, with Lead (Z = 82) providing the highest attenuation. Statistical analysis of radioactive decay confirmed a normal distribution with a standard deviation of 48.89 counts per minute, validating the reliability of the system for environmental surveys.

Keywords: GM Counter, Attenuation, Detection Efficiency, Absorption

1. Introduction
Nuclear safety concerns arising from industrial accidents and high-altitude cosmic radiation exposure have intensified the demand for reliable, portable radiation detectors [1, 2]. While advanced spectrometry systems exist, G-M counters remain the primary choice for operational monitoring in nuclear facilities due to their ruggedness [3, 4]. Evaluating its performance involves characterizing the counting plateau, detection efficiency for different radiations/energies, and the statistical behaviour of counts. Modern texts define the plateau as the nearly flat region of count rate vs. applied voltage; its length and slope indicate operating stability and aging [5]. For charged particles, GM intrinsic efficiency is high, but for gamma rays it is typically only 1- 5 % [6]. Efficiency depends strongly on tube geometry, wall material/thickness, and working gas [5, 7]. GM counts follow Poisson statistics; modern analysis tools (e.g., RadStat) automate mean, variance, distributions, and error propagation for GM datasets [5, 8]. However, empirical data regarding their response to low-level activities in liquid effluents is notably scarce [9]. This study aims to fill this gap by characterizing the counting statistics and absorption cross-sections of gamma and beta particles using the ST-350 counter system.

2. Methodology
The experimental investigations were carried out using a specialized radiation counting system consisting of an ST-350 counter, a G-M tube with a thin mica window, and a standard shelf stand for precise source positioning (see Fig 1). The methodology was divided into four distinct phases to characterize the detector's operational limits and its interaction with various radiation types.

Fig 1: ST350 setup with source and GM-Tube

2.1 Plateau Determination and Operating Voltage Selection

To ensure stable detector performance, the Geiger plateau was first identified to determine the optimal operating voltage. A gamma-emitting ^{137}Cs source (5 μCi) was placed in a lead castle at a fixed distance from the G-M tube window. Starting from an initial bias of 400 V, the high voltage (HV) was increased until the threshold voltage ($V_T \approx$ 640 V) was reached. From the threshold, counts (N) were recorded for 30 seconds, performed in triplicate at each 20 V increment. The voltage was increased until the count rate began to surge rapidly, indicating the continuous discharge region at approximately 980 V. The optimal operating voltage (V_{op}) was calculated as the midpoint of the stable plateau region (810 V), and all subsequent experiments were conducted at this potential.

2.2 Efficiency Calibration

The absolute efficiency of the G-M counting system was determined for alpha, beta, and gamma radiation using standard sources. Prior to source measurement, a background run was conducted to establish the ambient radiation level (s ≈ 79.33 counts). Three radioactive sources; ^{210}Po (1 μCi), ^{90}Sr (0.1 μCi), and ^{60}Co (1 μCi) were placed individually on the top shelf of the stand. Observed counts were corrected for background and compared against the theoretical disintegration rate calculated using the conversion factor 1 $\mu Ci = 2.22 \times 10^6$ dpm [10]. Equation (i) was used to calculate the calibration efficiency of the GM-tube.

$$\% \text{ Efficiency} = r\,(100)/CK \qquad \text{(i)}$$

Where r is the measured activity in *cpm*, C is the expected activity of the source in μCi,
and K is the conversion factor from 1 $Ci = 2.22 \times 10^{12}$ *dpm*.

2.3 Absorption Cross-Section and Material Dependence

This phase investigated the attenuation properties of gamma and beta radiation across different shielding materials and thicknesses. Absorbers including Plastic (poly-carbonate, Z = 6), Aluminum (Z = 13), and Lead (Z = 82) were utilized to evaluate atomic number dependence. A ^{137}Cs source was placed on the second shelf, and counts were recorded through absorbers of varying thicknesses (e.g., 0.032 cm to 0.250 cm for Lead). The procedure was repeated using a ^{90}Sr source to contrast the absorption profiles of charged particles versus photons. Each run was performed for a preset time of 60 seconds to ensure statistical consistency.

2.4 Statistical Analysis of Radioactive Decay

A counting statistics experiment was performed in order to validate the stochastic nature of nuclear processes [11]. To attain normalization, the ^{90}Sr source was positioned such that the observed count rate was approximately 2000 counts per minute. Once the distance was fixed, 40 separate 1-minute counts were recorded under identical conditions. The resulting data set was used to calculate the mean ($\bar{x}$), variance (S^2), and standard deviation (S) to determine if the process followed a normal (Gaussian) distribution (see Table 3).

Taking the background count = 54/s ==> 54cpm and N = 40, standard deviation (S) was calculated using the formulation below:

$$\sum x_i = 73480 \text{ counts.}$$

$$Average\ (\bar{x}) = \frac{\sum x_i}{N} = 1837$$

$$\sum(x_i - \bar{x})^2 = 93182$$

$$S^2 = \frac{1}{N-1}\Sigma(x_i - x)^2$$

$$s^2 = \frac{1}{39} \times 93182$$

$$S^2 = 2389.28$$

$$S = \sqrt{2389.28}$$

$$S = 48.89$$

3. Results and Discussion

3.1 Operating Characteristics

The G-M tube exhibited a threshold voltage of 640 V. The plateau region showed a stable count rate between 800 V and 980 V, after which continuous discharge was observed. The optimal operating voltage was established at 810 V (see Fig 2).

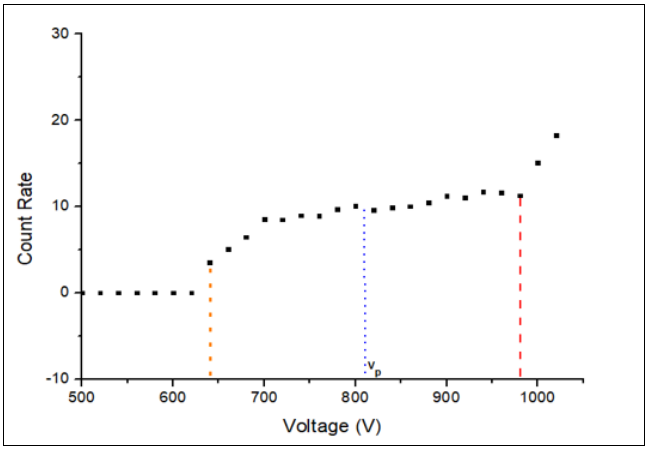

Fig 2: Geiger Plateau for determination of operating voltage

3.2 Detection Efficiency

The results for the Geiger-Müller (G-M) counter efficiency revealed significantly low values: 0.003% for ^{210}Po, 0.08% for ^{90}Sr, and 0.02% for ^{60}Co. These findings deviate from the theoretical ideal mentioned in the literature, which suggests that G-M counters can achieve near 100% efficiency for charged particles [6-9]. This discrepancy highlights critical differences between intrinsic and absolute efficiency in practical applications. Theoretical principles state that the Geiger counter excels at detecting charged particles (Alpha and Beta) because they directly ionize the gas molecules (Helium or Argon) within the tube [12]. However, the efficiency for the alpha source (^{210}Po) was the lowest (0.003%). This is attributed to the low penetration of alpha particles, which likely suffered significant attenuation before reaching the active volume of the gas, despite the tube's thin mica window.

Beta vs. Gamma Efficiency

Although the beta efficiency (0.08%) is higher than other sources, it remains low compared to the 100% theoretical interaction probability for charged particles [13]. This is likely due to the "weakness in the activity counts" and the age of the sources, which were purchased since 10 years ago. As can be seen in Table 1, for the gamma efficiency (0.02%); theoretically, gamma rays are photons that travel as quanta at the speed of light and are difficult to capture in low-density gases [14]. Because the gas inside the tube is not very dense, most gamma radiation passes through without producing the necessary electron-ion pairs for a count [15]. The system showed the highest efficiency for Beta particles (^{90}Sr at 0.08 %) compared to Gamma (^{60}Co at 0.02 %). The low intrinsic efficiency is primarily due to the low density of the Helium/Argon gas fill, which allow photons to pass without interaction.

Table 1: GM tube calibration efficiency data

Radioactive Source	Counts			Average Counts	Corr. Counts	Efficiency (%)
Po-210	67	62	65	64.67	- 14.66	0.003
Sr-90	1848	1867	1828	1847.67	1768.34	0.08
Co-60	374	377	366	372.33	293.00	0.02

3.3 Absorption Cross-Section and Material Dependence

Gamma ray (^{137}Cs) absorption followed an exponential decay law relative to thickness. As shown in Table 2, Lead (Z = 82) demonstrated significantly lower corrected counts (560.33) compared to Aluminum (655.33) for gamma radiation, confirming that higher atomic number materials increase the probability of photoelectric and Compton interactions [16, 17]. The attenuation of beta particles (^{90}Sr) similarly followed an exponential decay trend relative to the thickness of the absorber, though with significantly higher sensitivity to material density compared to gamma radiation. As shown in Table 3, transitioning from a low-Z material such as Plastic (Z = 6) to Aluminum (Z = 13) resulted in a sharp decrease in corrected counts from 1043.00 to 352.33. When Lead (Z = 82) was employed, the particles were effectively stopped, with corrected counts falling below detectable background levels (recorded as -21). This behaviour confirms that beta particles, as charged electrons, lose energy much more rapidly than gamma photons through a combination of inelastic collisions with atomic electrons and radiative processes known as bremsstrahlung [18].

Table 2: Gamma-ray counts with varying absorber atomic numbers

Absorbers	Atomic Number	Counts 1st	2nd	3th	Average	Corr. Counts	ln (Counts)
Plastic	6	714	775	727	738.67	656.67	6.4872
Aluminium	13	760	721	731	737.33	655.33	6.4851
Lead	82	658	632	637	642.33	560.33	6.3285

Table 3: Beta particles count with varying absorber atomic numbers

Absorbers	Atomic Number	Counts 1st	2nd	3th	Average	Corr. Counts	Ln (Counts)
Plastic	6	1123	1132	1120	1125.00	1043.00	6.9498
Aluminium	13	479	431	393	434.33	352.33	5.8646
Lead	82	66	55	62	61	- 21	0.0000

3.4 Statistical Reliability

The mean count rate was 1837 cpm with a variance of 2389.28. The calculated standard deviation (S = 48.89) suggests that 68 % of measurements fall within the ±1σ range, consistent with Poisson statistics for high count rates [8].

Table 4: Statistical data for radioactive decay of ^{90}Sr over forty independent observations

N	x_i (cpm)	$(x_i - \bar{x})$	$(x_i - \bar{x})^2$
1	1801	−36	1296
2	1859	+ 22	484
3	1921	+ 84	7056
4	1790	−47	2209
5	1784	−53	2809
6	1790	−47	2209
7	1856	+ 19	361
8	1850	+ 13	169
9	1752	−85	7225
10	1891	+ 54	2916
11	1817	−20	400
12	1830	−7	49
13	1826	−11	121
14	1877	+ 40	1600
15	1893	+ 56	3136
16	1837	00	00
17	1763	−74	5476
18	1842	+ 5	25
19	1814	−23	529
20	1838	+ 1	1
21	1914	+ 77	5929
22	1905	+ 68	4624
23	1850	+ 13	169
24	1853	+ 16	256
25	1857	+ 20	400
26	1849	+ 12	144
27	1866	+ 29	841
28	1798	− 39	1521
29	1818	− 19	361
30	1859	+ 22	484
31	1793	− 44	1936
32	1915	+ 78	6084
33	1799	− 38	1444
34	1876	+ 39	1521
35	1915	+ 78	6084
36	1715	−122	14884
37	1811	−26	676
38	1885	+ 48	2304
39	1794	− 43	1849
40	1777	− 60	3600

4. Conclusion

This study successfully characterized the operational limits and detection capabilities of the ST-350 G-M counter system. While the device exhibits low absolute efficiency for gamma rays, its predictable statistical behavior and clear response to material shielding make it a viable tool for low-level radiation surveys and educational applications. In conclusion, the study confirmed that the G-M counter is more efficient for beta particles (^{90}Sr) than for gamma rays (^{60}Co).

5. References

1. Marques L, Vale A, Vaz P. State-of-the-art mobile radiation detection systems for different scenarios. Sensors. 2021; 21(4):1051.
2. Vetter K. The nuclear legacy today of Fukushima. Annual Review of Nuclear and Particle Science. 2020; 70(1):257-292.
3. Abele J. Watchdog of the Atomic Age-The Geiger-Müller Counter in the History of Radiation Protection. Metrology Throughout the Ages, 55.
4. Nagamani SM. Radiation Monitoring Systems-Current Trends. In Nuclear Instrumentation and Control. Singapore: Springer Nature Singapore, 2025, 1-50.
5. Owens A, Peacock A. Compound semiconductor radiation detectors. Nuclear Instruments and Methods in Physics Research Section A: Accelerators, Spectrometers, Detectors and Associated Equipment. 2004; 531(1-2):18-37.
6. Arbutina D, Vasić-Milovanović A, Nedić T. Statistical methods for designing a Geiger-Muller counter suitable for an early warning system. Nuclear Instruments and Methods in Physics Research Section A: Accelerators, Spectrometers, Detectors and Associated Equipment. 2022; 1040:167268. Doi: https://doi.org/10.1016/j.nima.2022.167268
7. Arbutina D, Vasić-Milovanović A, Nedić T. The influence of the GM tube insulation parameters on the GM counter characteristics. Vacuum. 2022; 196:110755. Doi: https://doi.org/10.1016/j.vacuum.2021.110755
8. Shahmohammadi Beni M, Watabe H, Kwan WS, Islam MR, Yu KN. RadStat: An open-source statistical analysis tool for counts obtained by a GM counter. Plos One. 2022; 17(5):e0267610. Doi: https://doi.org/10.1371/journal.pone.0267610
9. Obrenović MD, Janićijević AJ, Arbutina DS. Statistical review of the insulation capacity of the Geiger-Muller counter. Nuclear Technology and Radiation Protection. 2018; 33(4):369-374.
10. Wolfe RR, Chinkes DL. Isotope tracers in metabolic research: Principles and practice of kinetic analysis. John Wiley & Sons, 2004.
11. Yuan X. Stochastic modeling of deterioration in nuclear power plant components. Waterloo, ON, Canada: University of Waterloo, 2007.
12. Riggi F. Educational and amateur Geiger counter experiments: 50+ activities for beginners and beyond. Springer Nature, 2024. Doi: https://doi.org/10.1007/978-3-031-56960-9
13. Podgoršak EB. Interactions of charged particles with matter. In Radiation physics for medical physicists. Cham: Springer International Publishing, 2016, 229-276.
14. Puputti HJ. Gamma-rays in low-background facilities: Fundamentals of spectra measurement and energy calibration at Callio Lab (Master's thesis, H. Puputti), 2022.
15. Pathak A. Measurement of Radiation. In Tools and Techniques in Radiation Biophysics. Singapore: Springer Nature Singapore, 2023, 109-162.
16. Riggi F. Radiation interaction. In Educational and Amateur Geiger Counter Experiments: 50+ Activities for Beginners and Beyond. Cham: Springer Nature Switzerland, 2024, 23-36.
17. Singh MP, Sandhu BS, Singh B. Measurement of the effective atomic number of composite materials using Rayleigh to Compton scattering of 279 keV gamma rays. Physica Scripta. 2007; 76(4):281.
18. Amusia MY. Atomic Bremsstrahlung: Retrospectives, current status and perspectives. Radiation Physics and Chemistry. 2006; 75(10):1232-1250.